RSC Advances

PAPER

View Article Online
View Journal | View Issue

Cite this: *RSC Adv.*, 2026, **16**, 13135

Fabrication of self-assembled CuO nanosheets for the sustainable synthesis of 2-substituted 1,3-benzothiazoles

Praveen Kumar Atal,[a] Bhaskar Dwivedi,[b] Diksha Bhardwaj, *[c] Debanjan Guin [d] and Deepika Choudhary *[a]

We report the rapid, sustainable, facile, environmentally friendly synthesis of copper oxide nanosheets (CuO NSs) and their application as a nanocatalyst for the synthesis of 2-substituted 1,3-benzothiazoles. The CuO NSs were characterized by various analytical techniques, including UV-Vis, fourier transform infrared spectroscopy (FT-IR), X-ray diffraction (XRD), scanning electron microscopy (SEM), transmission electron microscopy (TEM), and energy-dispersive X-ray spectroscopy (EDS) mapping. CuO NSs were successfully utilized in the environmentally-friendly synthesis of biologically active 2-substituted 1,3-benzothiazole derivatives in an aqueous ethanol medium. The desired products were obtained in excellent yields without the formation of side products. The synthetic efficacy of this compound is underscored by its high-yielding protocol across a diverse range of substrates and ability to operate under mild reaction conditions. The nanosheet morphology of CuO provides abundant active sites, enabling exceptional catalytic efficiency. The catalyst is readily recoverable and reusable over multiple cycles without significant loss of activity. This operationally simple strategy combines high atom economy, excellent recyclability, and environmentally benign conditions, offering a valuable route to benzothiazole frameworks of pharmaceutical and industrial relevance.

Received 9th February 2026
Accepted 2nd March 2026

DOI: 10.1039/d6ra01164k

rsc.li/rsc-advances

1. Introduction

N-heterocyclic compounds are among the most fascinating classes of organic molecules, serving as the structural backbone for a vast range of natural products, pharmacologically active agents, and fine chemicals. Their unique cyclic frameworks impart distinctive physicochemical properties and versatile reactivity.[1–3] These features make *N*-heterocycles indispensable in medicinal, agricultural, and material sciences. Among the various *N*-heterocyclic frameworks, benzothiazoles hold a prominent place due to their rigid, electron-rich fused thiazole–benzene structure. The carbon atom positioned between the nitrogen and sulfur atoms serves as a highly reactive site, enabling diverse functionalization. 2-Substituted benzothiazoles, in particular, manifest a broad spectrum of biological activities, including anticonvulsant,[4] antimicrobial,[5] antioxidant,[6] antiviral,[7] anti-inflammatory,[8] antituberculosis,[9] anticancer,[10] antidepressant,[11] antidiabetic,[12] anti-HIV,[13] analgesic,[14] and microbicidal properties.[15] Their pharmacological versatility has made them key scaffolds in drug discovery. Fig. 1 showcases representative drugs incorporating the 2-substituted benzothiazole moiety, reflecting the structural diversity and application breadth of this pharmacophore.[16]

Beyond medicinal applications, benzothiazole derivatives also play vital roles in industrial sectors, functioning as corrosion inhibitors,[17] dyes,[18] polymer additives,[19] pesticides,[20] textile auxiliaries,[21] and vulcanization accelerators.[22] Furthuremore, in materials science, they serve as antioxidants, dopants in electroluminescent devices, and chemosensors due to their favorable photophysical and electrochemical properties.[23]

Owing to their key importance in several applications, 2-substituted 1,3-benzothiazoles have been synthesized *via* several strategies, including the condensation of 2-aminothiophenols with aldehydes,[24] acid chlorides,[25] esters,[26] and carboxylic acids,[27] as well as through Jacobson's cyclization of thiobenzanilides.[28] Among these, the condensation of 2-aminothiophenols with aldehydes is the most widely utilized due to its operational simplicity and broad substrate scope. Various catalysts and reagents have been reported for this condensation, including alkyl carbonic acid,[29] PI–Pt,[30] CuI,[31] ABMs–$ZnBr_2$,[32] PEG-400,[33] SiO_2–Cu NPs,[34] nano-CeO_2,[35] and CdS nanoparticles[36] among others. Although these protocols have contributed significantly to the field, certain approaches may

[a]*Department of Chemistry, University of Rajasthan, Jaipur, Rajasthan, India. E-mail: deepika028@gmail.com*

[b]*Department of Chemistry, S. R. K. Government College Begun, Chittorgarh, Rajasthan, India*

[c]*Department of Chemistry, S. S. Jain Subodh PG College, Jaipur, Rajasthan, India. E-mail: dikshabhardwaj00@gmail.com*

[d]*Department of Chemistry, Institute of Science, Banaras Hindu University Varanasi, Uttar Pradesh, India*

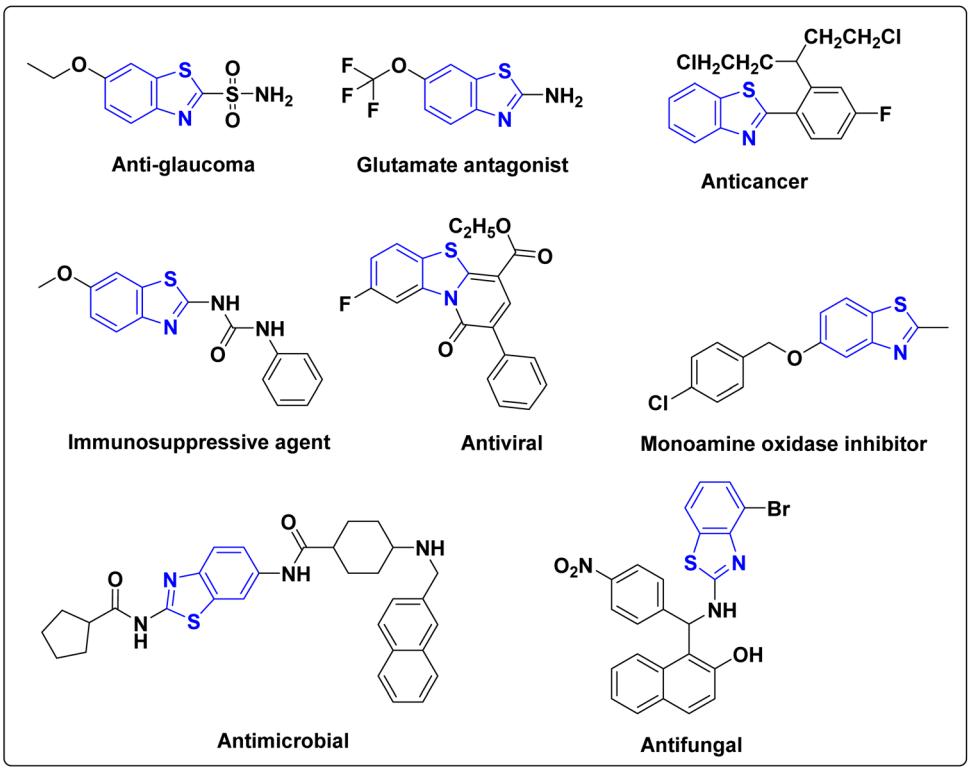

Fig. 1 Pharmacologically important benzothiazole scaffolds.

still involve challenges such as moderate yields, stringent reaction conditions, higher catalyst loading, costly materials, use of organic solvents, longer reaction times, or multistep work-up procedures. Addressing these challenges requires the development of eco-friendly, efficient, and reusable catalytic systems capable of operating under mild and green conditions.

Nanostructured catalysts, including nanoparticles and metal-oxide nanosheets, have emerged as highly effective in heterocyclic synthesis due to their large surface area, enhanced reactivity, high chemical stability, and excellent recyclability over multiple cycles.[37] The metal-oxide nanosheet morphology provides a high density of exposed active sites and a large accessible surface area. This facilitates effective interaction between the catalyst and reactants, thereby accelerating the reaction and improving conversion under mild conditions.[38] Nanosheets possess a two-dimensional structure with a very high aspect ratio, which exposes a greater proportion of surface atoms for catalytic interactions. This increased density of accessible active sites enables enhanced substrate adsorption and activation.[39] Moreover, nanosheets can provide anisotropic surface chemistry, where specific crystal facets with higher catalytic activity are preferentially exposed, leading to improved performance even under mild conditions.[40] Consequently, CuO NSs emerge as a highly promising system, as their unique morphology offers distinct catalytic advantages compared to conventional nanoparticles. The flat, extended surfaces of CuO NSs also facilitate better contact between reactants and catalyst, enhancing reaction kinetics.[41] These structural and surface characteristics collectively explain the superior performance of CuO NSs as catalyst in various chemical processes.

Furthermore, water as the reaction medium offers several advantages in organic synthesis combines environmental sustainability with high efficiency. Its polarity aids in dissolving reactants and improving heat transfer, while hydrogen bonding stabilizes transition states, enhancing reaction rate and selectivity.[42] The use of ultrasound irradiation in water as the reaction medium offers significant advantages in catalytic processes by enhancing mass transfer and promoting efficient mixing through acoustic cavitation.[43] Water, as a green and non-toxic solvent, further improves sustainability and facilitates catalyst dispersion; moreover, the use of a water–ethanol solvent system enhances solubility of organic substrates while maintaining environmental compatibility, making ultrasound-assisted aqueous catalysis an environmentally benign and highly efficient approach. Growing environmental concerns have driven substantial interest in the design of sustainable and eco-friendly synthetic methodologies. Within this framework, we report a facile, scalable and sustainable synthesis of CuO NSs and utilises its catalytic efficiency in the synthesis of bioactive 2-substituted 1,3-benzothiazole derivatives *via* condensation of 2-aminothiophenol with substituted aromatic aldehydes in aqueous ethanol medium. This method proceeds under mild conditions, avoids toxic solvents, minimizes waste, and delivers excellent yields within minutes, demonstrating a green, and industrially relevant protocol for the synthesis of biologically and industrially important benzothiazole scaffolds.

2. Results and discussion

After the fabrication of the CuO NSs *via* direct calcination method, the structure of this nanosheets fully characterized by a number of spectroscopic techniques including UV-Vis, FT-IR, XRD, TEM, SEM and, EDS.

2.1. UV-visible absorption spectra analysis

The absorption spectrum of the synthesized CuO NSs was recorded at room temperature using a UV-Vis spectrophotometer in the 200–800 nm wavelength range (Fig. 2a). A distinct absorption peak observed at 367 nm corresponds to the characteristic charge transfer transition of CuO nanostructures. This result is consistent with earlier studies, where similar peaks were reported around 360–380 nm for CuO synthesized *via* thermal and green methods.[44,45] The observed absorption confirms the successful formation of nanoscale CuO. The optical energy band gap of the synthesized CuO NSs was determined using a Tauc plot (Fig. 2b), where $(\alpha h\nu)^2$ is plotted against $h\nu$ based on the equation:[46]

$$(\alpha E_{\text{photon}})^2 = K(E_{\text{photon}} - E_g)$$

Here, α represents the absorption coefficient, $E_{\text{photon}} = h\nu$ is the photon energy, K is a constant, and E_g denotes the optical band gap. The Tauc plot derived from UV-Vis absorption data shows an apparent optical band gap of approximately 2.94 eV for the CuO NSs. This blue-shifted absorption edge compared to bulk CuO may be attributed to nanoscale effects, surface defects, or higher-energy electronic transitions rather than the intrinsic band gap.

2.2. FT-IR analysis

The FT-IR spectrum of the synthesized CuO NSs was recorded in attenuated total reflectance (ATR) mode to analyze the functional groups and confirm the formation of the metal oxide, as presented in Fig. 3. The spectrum displayed distinct absorption bands at 593 cm^{-1}, 523 cm^{-1}, and 471 cm^{-1}, corresponding to the Cu–O stretching vibrations characteristic of the monoclinic phase of CuO, in agreement with reported literature.[47] In addition, a peak at 639 cm^{-1} is attributed to the formation of Cu–O bonds.[48] Broad bands observed at 3785 cm^{-1} and 3699 cm^{-1} are assigned to O–H stretching vibrations, attributed to surface hydroxyl groups or adsorbed water molecules on the nanosheet surface features commonly observed in nanostructured metal oxides.[49] The absorption bands at 1368 cm^{-1} and 1216 cm^{-1} are associated with C–H bending and C–N/C–O stretching vibrations, respectively, likely arising from residual organic species or synthesis precursors. Overall, the FT-IR analysis confirms the successful formation of CuO NSs.

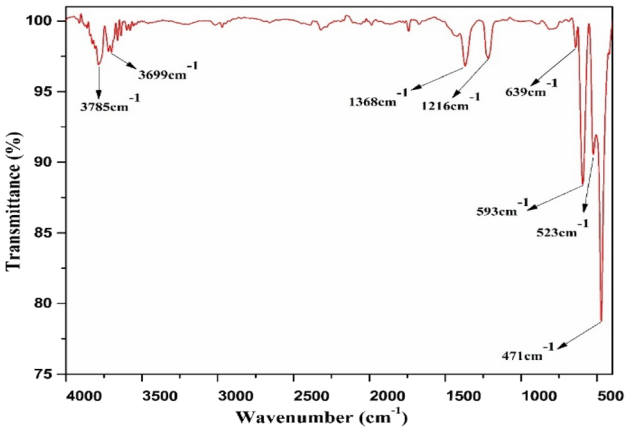

Fig. 3 FT-IR spectrum of CuO NSs.

2.3. XRD analysis

The XRD pattern of the synthesized CuO NSs is shown in Fig. 4. The diffraction peaks in Bragg's angles $2\theta = 32.5°$, 35.5°, 38.7°, 46.3°, 48.8°, 53.5°, 58.3°, 61.6°, 66.3°, 68.0°, 72.4°, and 75.1°

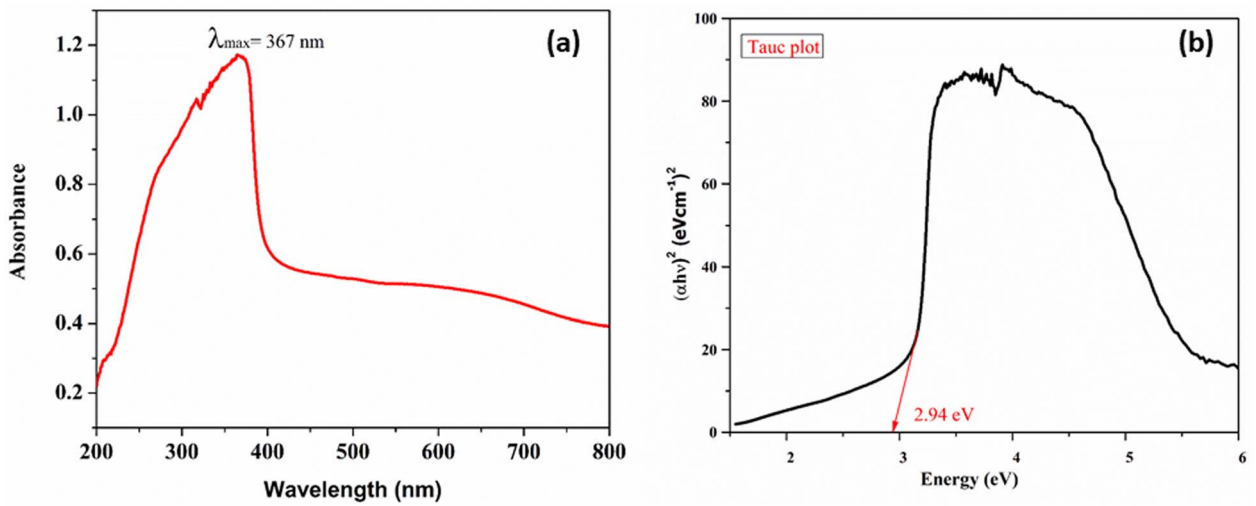

Fig. 2 (a) UV-Visible spectrum of CuO NSs; (b) Tauc plot of CuO NSs.

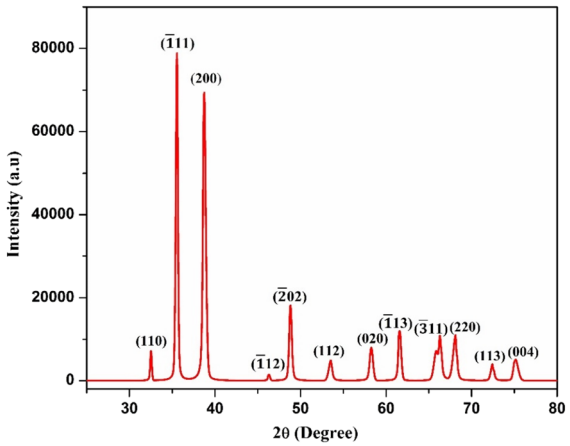

Fig. 4 XRD pattern of CuO NSs.

correspond to the (110), (111), (200), (112), (202), (020), (202), (113), (311), (220), (113), and (004) crystal planes, respectively, which are characteristic of the monoclinic phase of copper(II) oxide. The diffraction pattern closely matches the standard data from JCPDS Card No. 48-1548,[50] confirming the formation of phase-pure and highly crystalline CuO with a monoclinic crystal structure. The crystallite size was calculated using Scherrer's equation ($D = 0.9\lambda/\beta \cos\theta$). In this equation, λ is the wavelength of Cu Kα radiation (0.154 nm), θ is the Bragg angle corresponding to the most intense diffraction peak (35.5°), and β is the full width at half maximum (FWHM) of that peak. The average crystallite size of CuO NSs was estimated to be ~15 nm.

2.4. SEM and EDS analysis

The morphology and size of the synthesized CuO NSs were examined using SEM, as shown in Fig. 5a and b. The images revealed thin, sheet-like nanostructures with wrinkled surfaces that were loosely stacked, forming a porous network. During the synthesis process, the formation of CuO NSs is initiated by the generation of primary CuO nuclei, which subsequently undergo lateral growth through an aggregation-driven self-assembly mechanism. To minimize surface energy, these nuclei preferentially assemble in a two-dimensional manner, leading to the development of sheet-like architectures.[51] With continued reaction time, the assembled units merge and reorganize, resulting in well-defined CuO NSs, consistent with the SEM observations. The EDS analysis further confirms the elemental composition of the synthesized nanosheets, with no detectable impurity elements (Fig. 5e). The spectrum shows the presence of only copper (Cu) and oxygen (O) as the major elements, exhibiting a near-unity Cu/O atomic ratio, indicative of phase-pure CuO. Moreover, elemental mapping (Fig. 5c and d) demonstrates a uniform and homogeneous distribution of Cu and O throughout the nanosheet structure, further confirming the successful formation of phase-pure CuO NSs.

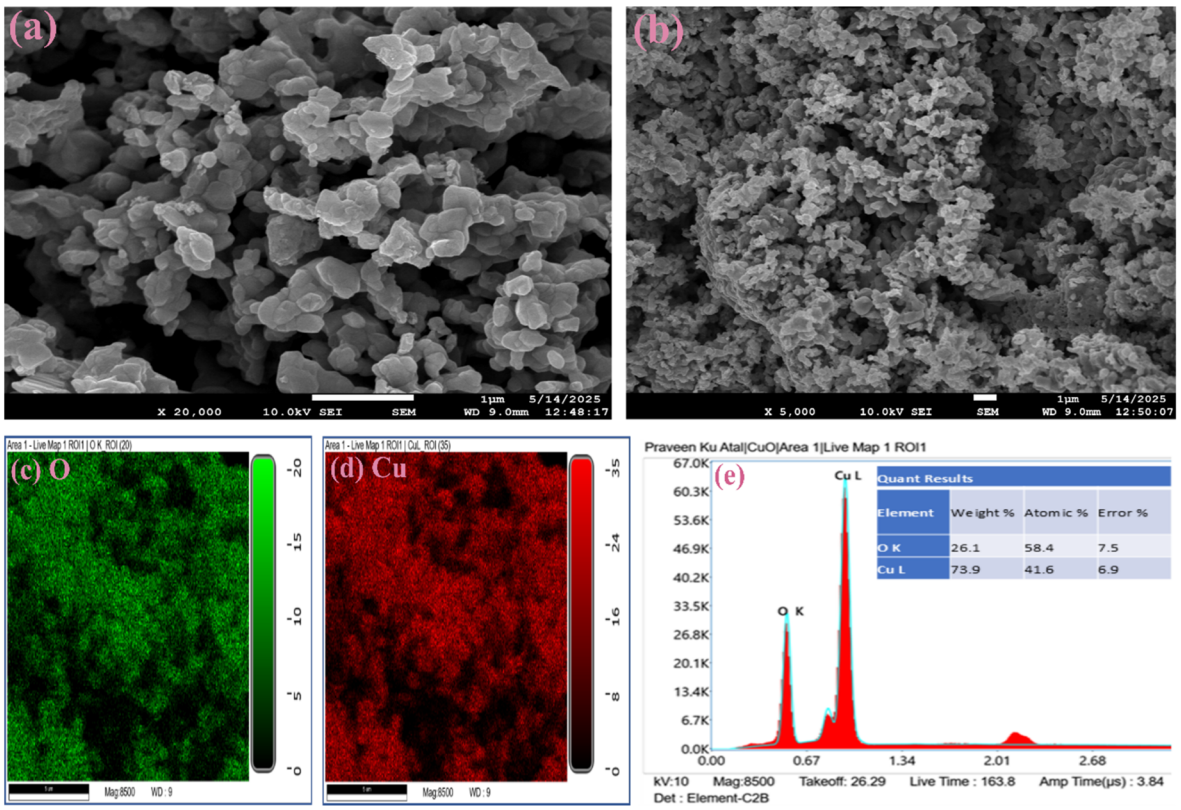

Fig. 5 SEM images of CuO NSs: (a) 1 μm (high-magnification) and (b) 1 μm (low-magnification) with elemental mapping of (c) O element and (d) Cu element. (e) EDS spectral (inset: atomic percentage of elements) plot of CuO NSs.

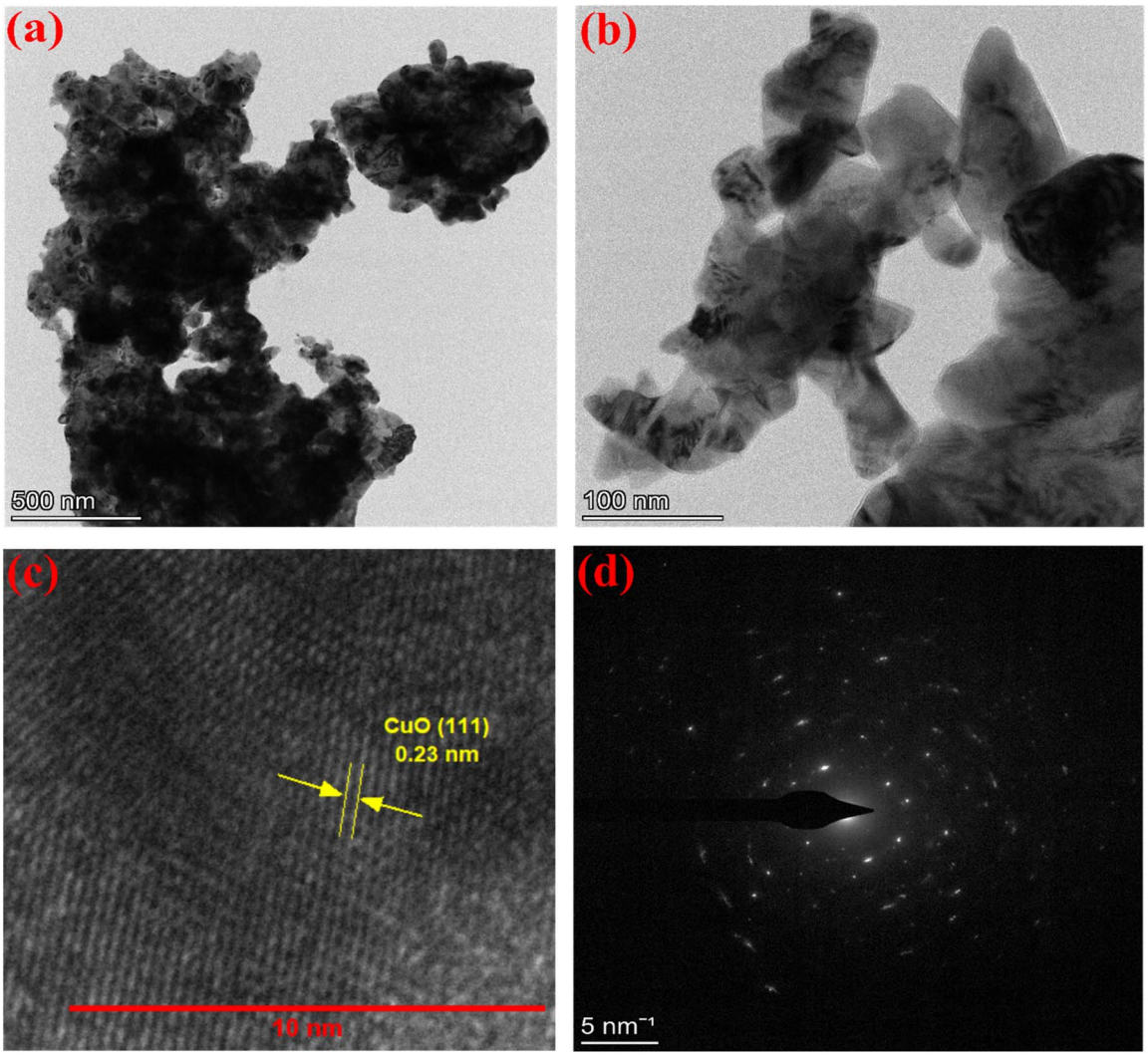

Fig. 6 TEM images of CuO NSs: (a) at a scale of 500 nm, (b) at a scale of 100 nm, (c) image at 10 nm showing lattice fringes, and; (d) SAED pattern of CuO NSs.

Table 1 The optimization of reaction conditions for synthesis of 2-substituted 1,3-benzothiazole derivatives[a]

Entry	Catalyst	Solvent	Temp. (°C)	Time (min)	Yield[b] (%)
1	—	—	80	100	—
2	—	H_2O	80	100	—
3	CuO (0.1 mmol)	—	80	60	55
4	CuO (0.1 mmol)	H_2O	r.t	60	70
5	CuO (0.1 mmol)	EtOH	r.t	60	64
6	CuO (0.1 mmol)	H_2O : EtOH (1 : 1)	r.t	60	82
7	CuO (0.1 mmol)	CH_3CN	r.t	120	Trace
8	CuO (0.1 mmol)	DMF	r.t	120	Trace
9	**CuO (0.125 mmol)**	**H_2O:EtOH (1:1)**	**r.t**	**10**	**94**
10	CuO (0.2 mmol)	H_2O : EtOH (1 : 1)	r.t	10	94
11	CuO (0.125 mmol)	H_2O : EtOH (1 : 1)	50	10	92
12	CuO (0.125 mmol)	H_2O : EtOH (1 : 1)	70	10	93
13	Fe_3O_4 (0.125 mmol)	H_2O : EtOH (1 : 1)	r.t	10	57
14	DABCO (0.125 mmol)	H_2O : EtOH (1 : 1)	r.t	10	35

[a] 2-aminothiophenol (1 mmol), benzaldehyde (1 mmol), and CuO NSs. [b] Isolated yield.

2.5. TEM analysis

The TEM analysis of the CuO nanocatalyst further validated the well-defined morphology and revealed clear lattice fringes, indicating a high degree of crystallinity. The TEM images of the synthesized nanostructures (Fig. 6a and b) shows nanosheet-like architectures in the fabricated sample. From the representative micrographs, the CuO NSs exhibits a highly crystalline, broken sheet-like morphology, with average width and length of 225 ± 80 nm and 181 ± 25 nm, respectively. The image shown in Fig. 6c reveals clear lattice fringes with an interplanar spacing of 0.233 nm, which can be indexed to the (111) crystallographic planes of CuO. The SAED pattern of the CuO NSs (Fig. 6d) displays sharp and well-defined concentric diffraction rings, confirming the high crystallinity of the synthesized CuO. Overall, these results confirm the successful synthesis of phase-pure, crystalline CuO NSs with favorable morphological characteristics, making them highly suitable for catalytic applications.

2.6. Catalytic activity of CuO NSs in the synthesis of 2-substituted 1,3-benzothiazole derivatives

Following the characterization of the CuO NSs, their catalytic performance was evaluated in the synthesis of 2-substituted 1,3-benzothiazole derivatives. To optimize the reaction conditions, the condensation of 2-aminophenol with benzaldehyde was selected as a model reaction. The effects of various parameters such as catalyst loading, solvent, temperature, and reaction time were systematically investigated and the results are summarized in Table 1. Initially, the model reaction was conducted both in the absence and in the presence of the catalyst to evaluate the catalytic efficiency of the CuO NSs. Subsequently, the reaction was performed in various solvents, including H_2O,

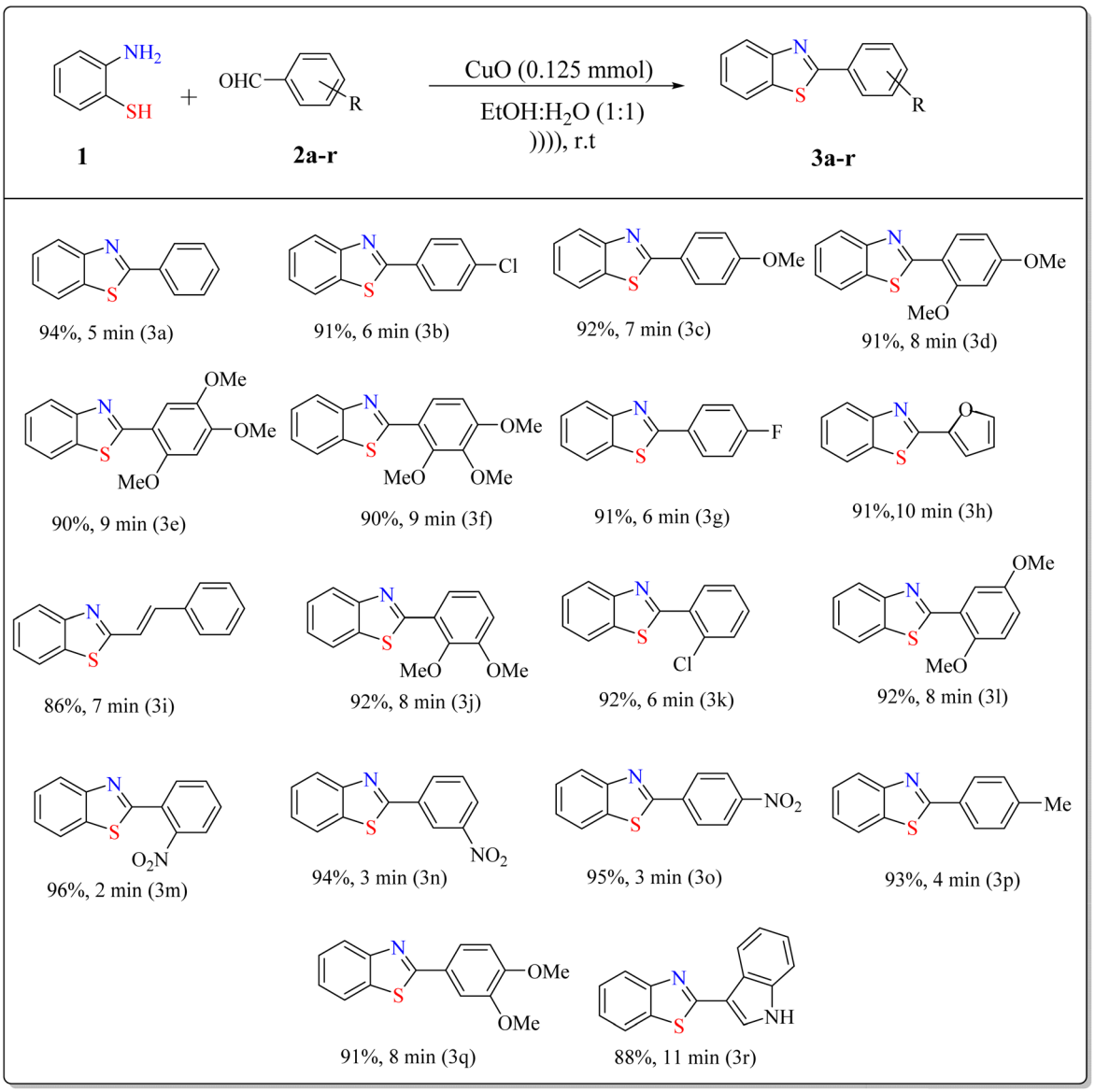

Scheme 1 Synthesis and substrate scope of 2-substituted 1,3-benzothiazole derivatives (**3a–r**).

EtOH, H_2O : EtOH, CH_3CN, and DMF, as well as under solvent-free conditions. As shown in Table 1, increasing the catalyst loading resulted in a significant improvement in both reaction time and yield (Table 1, entry 9). However, a further increase did not lead to any noticeable enhancement in reaction efficiency (Table 1, entry 10). Furthermore, the effect of temperature was investigated over a range from room temperature to 70 °C (Table 1, entries 9, 11, and 12). To further elucidate the role of CuO NSs as the catalyst, the model reaction was also carried out under identical conditions using Fe_3O_4 and DABCO as alternative catalysts (Table 1, entries 13, 14). The results clearly demonstrate that CuO NSs exhibit superior catalytic activity leading to enhanced reaction efficiency and product yield. The use of 0.125 mmol of CuO NSs as the catalyst in an H_2O : EtOH (1 : 1) solvent system at room temperature under ultrasound irradiation was identified as the optimal condition, offering a green reaction environment, a clean work-up procedure, and excellent product yield.

After the optimized reaction conditions, the substrate scope for the synthesis of 2-substituted 1,3-benzothiazole derivatives was subsequently explored. Various aromatic aldehydes with electron-donating and electron-withdrawing substituents were employed under the optimized reaction conditions to determine the efficacy of the CuO NSs as catalyst (Scheme 1). A wide variety of 2-substituted 1,3-benzothiazole derivatives were synthesized in high to excellent yields with short reaction time under environmentally benign conditions.

A plausible mechanism for the synthesis of 2-substituted 1,3-benzothiazoles catalyzed *via* CuO NSs is proposed in Scheme 2. Initially, CuO NSs activate the carbonyl group of aromatic aldehydes, facilitating its condensation with the amino group of 2-aminothiophenol to form an imine intermediate. Subsequently, intramolecular nucleophilic attack by the thiol group on the imine carbon leads to the formation of a dihydrobenzothiazole intermediate, followed by oxidation by molecular oxygen (air) to afford the aromatic 2-phenylbenzothiazole. The two-dimensional CuO NSs morphology provides a high density of exposed active sites and improved reactant-catalyst contact, which contributes to accelerated reaction rates. These nanosheets also expose catalytically active crystal facets that enhance efficiency under mild and environmentally benign conditions. In this study, the CuO NSs function as Lewis acidic centres that facilitate activation of the reactants and promote efficient cyclization for benzothiazole formation. The combination of high surface exposure and readily accessible active sites enhances substrate interaction, thereby improving the overall catalytic performance of CuO NSs under green reaction conditions.

The recyclability and reusability of CuO NSs were investigated under optimal conditions (Fig. 7). After completion of each reaction, the catalyst was readily recovered using centrifugation, thoroughly washed with ethanol, dried under vacuum, and reused in subsequent reaction cycles. The results demonstrated that the catalyst could be reused for up to eight consecutive cycles while maintaining excellent catalytic efficiency, with no noticeable decline in activity and morphology. A marginal decrease in product yield observed in the later cycles can be attributed to partial agglomeration of the CuO NSs during the reaction process. These findings confirmed that the reused catalyst exhibited remarkable structural stability and reusability highlighting the robustness of CuO NSs in the synthesis of 2-substituted 1,3-benzothiazole derivatives and their potential applicability in sustainable and green catalytic systems.

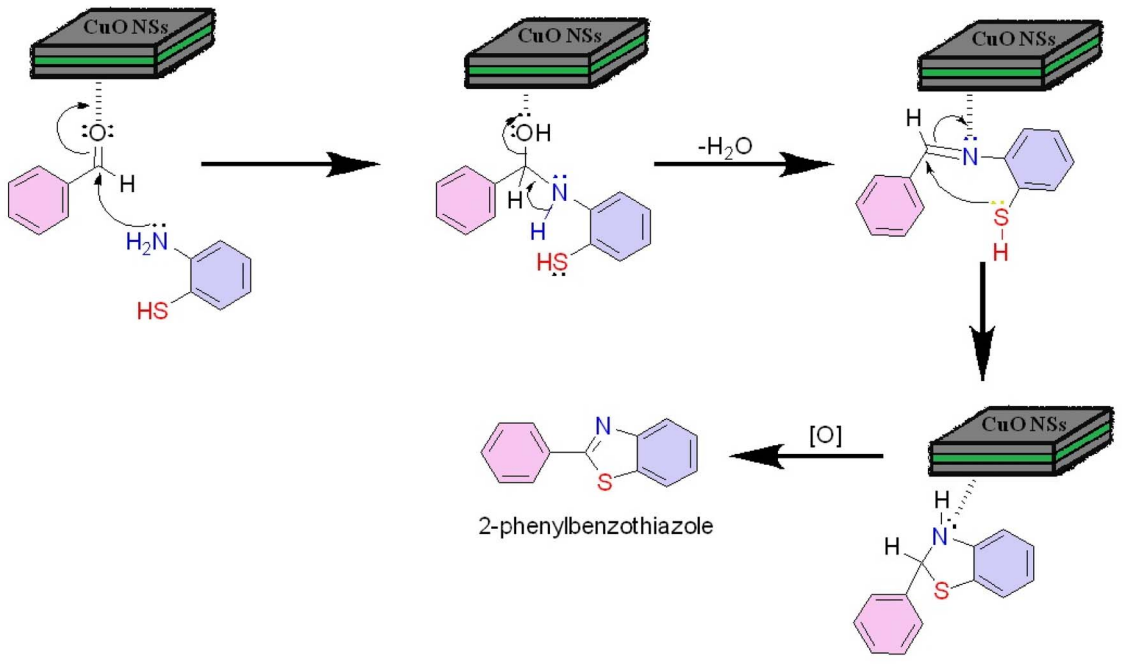

Scheme 2 Proposed mechanistic pathway for the CuO NSs catalyzed synthesis of 2-substituted 1,3-benzothiazole derivatives.

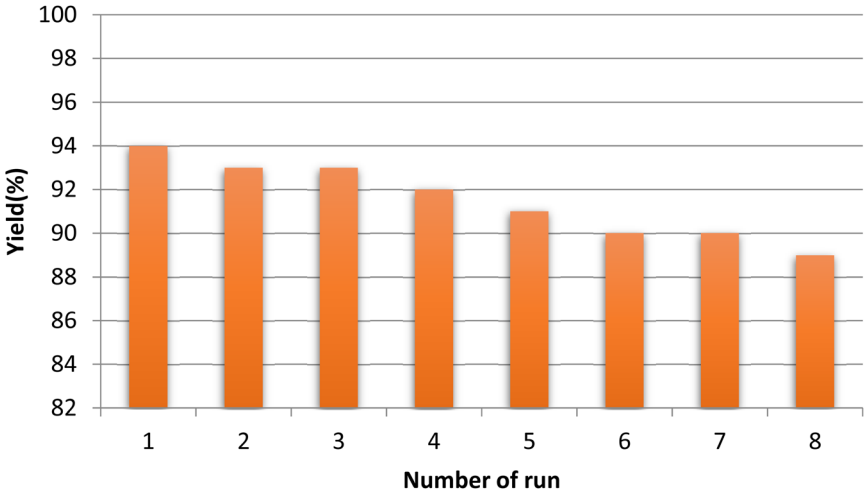

Fig. 7 Recyclability of CuO NSs for the synthesis of 2-substituted 1,3-beznothiozoles.

To investigate the possibility of copper leaching during the catalytic process, a hot filtration test[52] was performed under the optimized reaction conditions (Fig. 8c). In this experiment, the reaction mixture was passed through a preheated filter after 20 min to remove the catalytically active CuO NSs, and the resulting filtrate was then allowed to react for an additional 10 min. Monitoring of the reaction progress, together with metal analysis of the filtrate, confirmed negligible copper leaching, indicating the absence of homogeneous catalytic contribution. Furthermore, FT-IR spectrum (Fig. 8a) and SEM

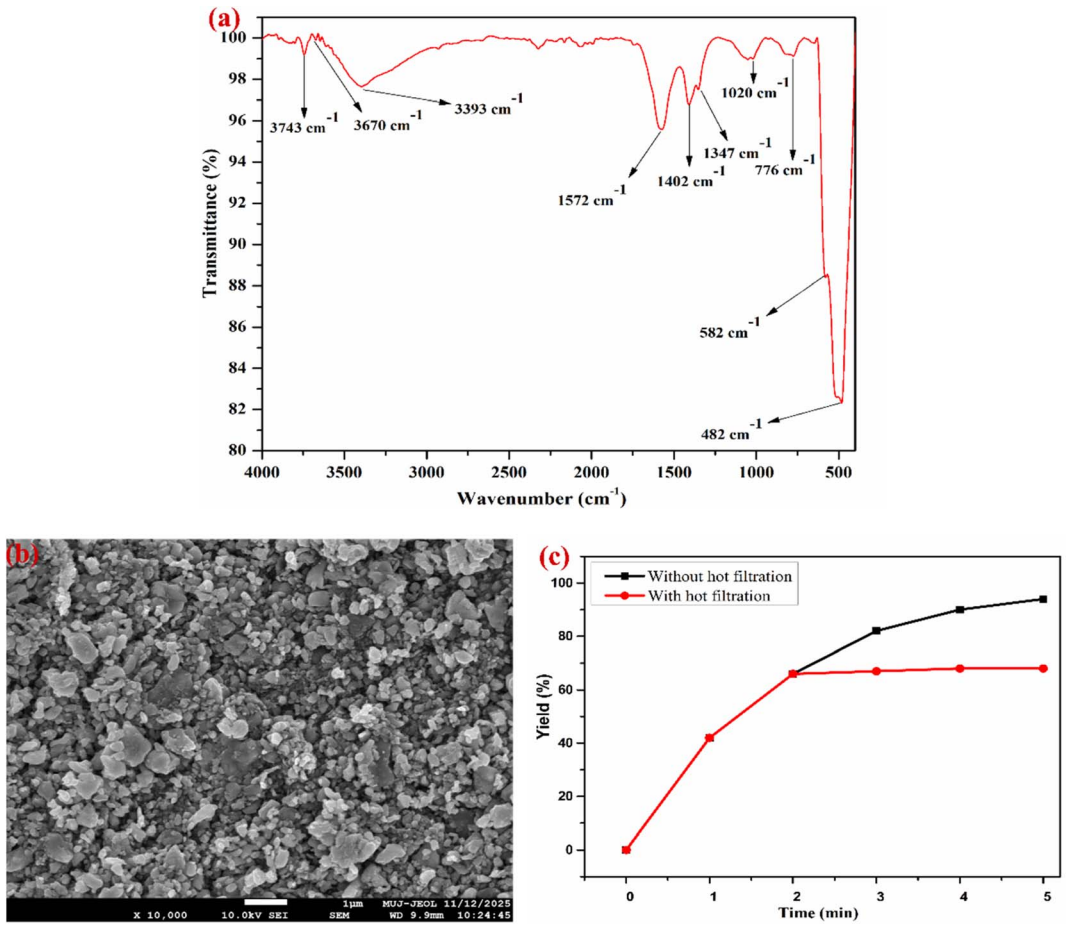

Fig. 8 (a) FT-IR spectrum of recycled CuO NSs (b) SEM image of recycled CuO NSs at 1 μm (c) hot filtration test.

Table 2 Comparison of reported catalytic systems for the synthesis of 2-substituted 1,3-benzothiazoles

Catalyst/System	Conditions	Time (h)	Yield	Ref.
Nano-BF_3/SiO_2	r.t, EtOH	25 min	90	53
Phosphonium acidic IL	Solvent-free, reflux, 120 °C	1 h	91	54
Cu(II)-glycerol/MCM-41	r.t, EtOH	2.5 h	96	55
Fe_3O_4@SiO_2@Cu–MoO_3	r.t, EtOH	2 h	98	56
CSA	r.t, EtOH : H_2O (1 : 1)	1 h	91	57
CuO NSs	r.t, EtOH : H_2O (1 : 1)	10 min	98	This work

image (Fig. 8b) of the recovered catalyst indicate the preservation of its structure and uniform nanosheet morphology after repeated use. These observations collectively demonstrate the excellent physicochemical stability of the catalyst during the reaction, enabling long-term storage and reuse without a significant loss in catalytic activity.

To further highlight the superior performance of the CuO NSs in benzothiazole synthesis, their catalytic activity was compared with previously reported catalysts (Table 2). The findings clearly show that the present catalyst demonstrates enhanced activity, shorter reaction times, and more favorable reaction conditions. Notably, these findings confirm the true heterogeneous nature and outstanding structural stability of the CuO NSs, underscoring their suitability for sustainable and reusable catalytic applications. This analysis reveals that the CuO NSs methodology outperforms previously reported systems in terms of speed, green solvent use, cost-effectiveness, and catalyst reuse, making it a superior and sustainable choice for the scalable synthesis of biologically and industrially relevant benzothiazole derivatives. The two-dimensional morphology of CuO NSs provides enhanced surface-active sites, enabling superior catalytic performance and making this protocol both industrially viable and environmentally sustainable.

3. Experimental section

3.1. Material and methods

All chemicals were purchased from Merck, Sigma-Aldrich, and TCI Chemical Companies and used without further purification. ^{1}H NMR (500 MHz) and ^{13}C NMR (100 MHz) spectra were recorded on a Bruker Avance spectrometer using $CDCl_3$ as the solvent and tetramethylsilane (TMS) as an internal standard. Fourier-transform infrared (FT-IR) spectra were recorded on a Bruker Alpha spectrometer in ATR mode over the range of 400–4000 cm^{-1}. X-ray diffraction (XRD) patterns were recorded on a Rigaku MiniFlex 600 diffractometer using Cu Kα radiation (λ = 0.15406 nm) over a 2θ range of 50–130°. Field-emission scanning electron microscopy (FE-SEM) and energy-dispersive X-ray spectroscopy (EDS) analyses were carried out on a JEOL JSM-7610FPlus equipped with an in-lens Schottky field emission gun and an EDAX detector.

3.2. Preparation of the CuO NSs

CuO NSs were prepared through the direct calcination of a copper nitrate and glucose mixture. Specifically, 1.25 g of copper nitrate [$Cu(NO_3)_2$] and 1.80 g of D-glucose were dissolved in 25 mL of distilled water in a 150 mL quartz beaker. The mixture was sonicated at 80 °C for 20 min, resulting in a viscous paste. The resulting paste was placed in a muffle furnace and calcined at 550 °C for 3 h to dehydrate the sample for subsequent investigation.

3.3. General procedure for the synthesis of 2-substituted 1,3-benzothiazole derivatives

CuO NSs (0.125 mmol) were added to a mixture of 2-aminothiophenol (1 mmol) and substituted aromatic aldehydes (1 mmol) in H_2O : EtOH (1 : 1). The mixture was stirred under ultrasonic waves at room temperature. After confirming reaction completion by TLC, ethyl acetate (2 mL) was added to extract the organic compounds, and the CuO NSs catalyst was separated *via* centrifugation. The product was purified by column chromatography using a 5 : 95 (v/v) ethyl acetate–hexane mixture. The catalyst was washed with ethanol and water, dried at 80 °C, and reused in subsequent catalytic cycles. Finally, the ^{1}H and ^{13}C-NMR spectroscopy were used to identify the products.

4. Conclusions

In this study, CuO NSs were successfully synthesized *via* a green and cost-effective method using environmentally benign precursors. The prepared CuO NSs were thoroughly characterized by various analytical techniques, confirming their crystalline and nanosheets morphology. The eco-friendly CuO NSs were successfully utilized as a heterogeneous catalyst for synthesizing 2-substituted 1,3-benzothiazole derivatives *via* reaction involving 2-aminothiophenol and substituted aromatic aldehydes in aqueous ethanol system under ambient conditions. The protocol demonstrated energy efficiency, excellent yields, high atom economy, easy separation of the catalyst, reusability, and operational simplicity within short reaction times. The CuO NSs structure exhibits outstanding surface characteristics and high purity, enhances its catalytic efficiency and selectivity adhering to green chemistry principles.

Author contributions

D. Choudhary: conceptualization, methodology, resources, funding, validation, software, supervision; D. Bhardwaj: writing – review & editing, visualization, investigation, conceptualization, supervision, methodology; D. Guin: investigation, resources, validation, B. Dwivedi: formal analysis, data

curation; PK Atal: writing – original draft, methodology, formal analysis, data curation.

Conflicts of interest

There are no conflicts to declare.

Data availability

The authors confirm that the data supporting the findings of this study are available within the article and its supplementary information (SI). Additional data are available from the corresponding author upon reasonable request. Supplementary information is available. See DOI: https://doi.org/10.1039/d6ra01164k.

Acknowledgements

The authors are grateful for the financial support of the SERB project [grant number SUR/2022/003899]. The authors thank Malaviya National Institute of Technology (MNIT) Jaipur, Banaras Hindu University (BHU), Varanasi, and Manipal University, Jaipur for the necessary instrument facilities.

References

1 D. K. Gour, Heterocyclic compounds: the diverse world of ringed molecules, *J. Med. Org. Chem.*, 2023, **6**, 108–110.
2 B. Gao, B. Yang, X. Feng and C. Li, Recent advances in the biosynthesis strategies of nitrogen heterocyclic natural products, *Nat. Prod. Rep.*, 2022, **39**, 139–162.
3 K. Mezgebe, Y. Melaku and E. Mulugeta, Synthesis and pharmacological activities of chalcone and its derivatives bearing N-heterocyclic scaffolds: a review, *ACS Omega*, 2023, **8**, 19194–19211.
4 B. Chauhan, R. Kumar, A. Mazumder, Salahuddin, H. Singh, R. K. Yadav and M. M. Abdullah, Updates on the synthetic strategies and structure–activity relationship of anticonvulsant benzothiazole and benzimidazole derivatives, *Lett. Drug Des. Discov.*, 2023, **20**, 1458–1482.
5 M. Singh, S. K. Singh, M. Gangwar, G. Nath and S. K. Singh, Design, synthesis and mode of action of novel 2-(4-aminophenyl)benzothiazole derivatives bearing semicarbazone and thiosemicarbazone moiety as potent antimicrobial agents, *Med. Chem. Res.*, 2016, **25**, 263–282.
6 E. N. Djuidje, R. Barbari, A. Baldisserotto, E. Durini, S. Sciabica, J. Balzarini, S. Liekens, S. Vertuani and S. Manfredini, Benzothiazole derivatives as multifunctional antioxidant agents for skin damage: structure-activity relationship of a scaffold bearing a five-membered ring system, *Antioxidants*, 2022, **11**, 407.
7 A. D. Borthwick, D. E. Davies, P. F. Ertl, A. M. Exall, T. M. Haley, G. J. Hart, D. L. Jackson, N. R. Parry, A. Patikis, N. Trivedi and G. G. Weingarten, ZnO nanoparticles: a green efficient catalyst for the room temperature synthesis of biologically active 2-aryl-1,3-benzothiazole and 1,3-benzoxazole derivatives, *J. Med. Chem.*, 2003, **46**, 4428.
8 J. Das, R. V. Moquin, J. Lin, C. Liu, A. M. Doweyko, H. F. DeFex, Q. Fang, *et al.*, Discovery of 2-amino-heteroaryl-benzothiazole-6-anilides as potent p56lck inhibitors, *Bioorg. Med. Chem. Lett.*, 2003, **13**, 2587–2590.
9 D. Alagille, R. M. Baldwin and G. D. Tamagnan, One-step synthesis of 2-arylbenzothiazole (BTA) and benzoxazole precursors for in vivo imaging of β-amyloid plaques, *Tetrahedron Lett.*, 2005, **46**, 1349–1351.
10 I. Hutchinson, M. S. Chua, H. L. Browne, V. Trapani, T. D. Bradshaw, A. D. Westwell and M. F. Stevens, Antitumor benzothiazoles. 14. Synthesis and in vitro biological properties of fluorinated 2-(4-aminophenyl) benzothiazoles, *J. Med. Chem.*, 2001, **44**, 1446–1455.
11 Ü. Demir Özkay, C. Kaya, U. Acar Çevik and Ö. D. Can, Synthesis and antidepressant activity profile of some novel benzothiazole derivatives, *Molecules*, 2017, **22**, 1490.
12 S. Sunil Kumar, D. S. Rathore, G. Gopal Garg, K. Kapil Khatri, R. Rahul Saxena and S. K. Sahu, Synthesis and evaluation of some benzothiazole derivatives as antidiabetic agents, *Int. J. Pharm. Pharm. Sci.*, 2017, **9**, 60.
13 Y. I. Asiri, A. Alsayari, A. B. Muhsinah, Y. N. Mabkhot and M. Z. Hassan, Benzothiazoles as potential antiviral agents, *J. Pharm. Pharmacol.*, 2020, **72**, 1459–1480.
14 K. R. Kumar, K. N. S. Karthik, P. R. Begum and C. M. Rao, Synthesis, characterization and biological evaluation of benzothiazole derivatives as potential antimicrobial and analgesic agents, *Asian J. Res. Pharm. Sci.*, 2017, **7**, 115–119.
15 M. K. Singh, R. Tilak, G. Nath, S. K. Awasthi and A. Agarwal, Design, synthesis and antimicrobial activity of novel benzothiazole analogs, *Eur. J. Med. Chem.*, 2013, **63**, 635–644.
16 S. R. Cheekatla, Benzothiazole-based therapeutics: FDA insights and clinical advances, *Chemistry*, 2025, **7**, 118.
17 A. Suhasaria, M. Murmu, S. Satpati, P. Banerjee and D. Sukul, Bis-benzothiazoles as efficient corrosion inhibitors for mild steel in aqueous HCl: molecular structure–reactivity correlation study, *J. Mol. Liq.*, 2020, **313**, 113537.
18 S. Harisha, J. Keshavayya, S. Prasanna and H. Joy Hoskeri, Synthesis, characterization, pharmacological evaluation and molecular docking studies of benzothiazole azo derivatives, *J. Mol. Struct.*, 2020, **1218**, 128477.
19 Z. Cao, F. Qiu, Q. Wang, G. Cao, L. Zhuang, Q. Shen and D. Yang, Synthesis of azo benzothiazole polymer and its application of 1 × 2 Y-branched and 2 × 2 Mach–Zehnder interferometer switch, *Optik*, 2013, **124**, 4036–4040.
20 G. Ma, Y. Zhang and X. Li, Dufulin enhances salt resistance of rice, *Pestic. Biochem. Physiol.*, 2022, **188**, 105252.
21 R. Avagyan, G. Luongo, G. Thorsén and C. Östman, Benzothiazole, benzotriazole, and their derivates in clothing textiles—a potential source of environmental pollutants and human exposure, *Environ. Sci. Pollut. Res.*, 2015, **22**, 5842–5849.
22 R. Reshmy, R. Nirmal, S. Prasanthkumar, K. K. Thomas, M. Thomas, T. M. Nair and A. Sulekha, Effect of benzothiazoloylthiazoles as secondary accelerators in the

sulfur vulcanization of natural rubber, *Rubber Chem. Technol.*, 2011, **84**, 88–100.

23 M. Nemiwal, T. C. Zhang and D. Kumar, Enzyme immobilized nanomaterials as electrochemical biosensors for detection of biomolecules, *Enzyme Microb. Technol.*, 2022, **156**, 110006.

24 Y. Xu, N. Zhao, F. Li, H. Xie, J. Wu, C. Wang and L. Wang, Efficient synthesis of 2-aryl benzothiazoles mediated by *Vitreoscilla* hemoglobin, *Mol. Catal.*, 2022, **533**, 112784.

25 (*a*) I. R. Laskar and T. M. Chen, *Chem. Mater.*, 2004, **16**, 117; (*b*) R. N. Nadaf, S. A. Siddiqui, T. Daniel, R. J. Lahoti and K. V. Srinivasan, *J. Mol. Catal. A: Chem.*, 2004, **214**, 155.

26 H. Matsushita, S. H. Lee, M. Joung, B. Clapham and K. D. Janda, Smart cleavage reactions: the synthesis of benzimidazoles and benzothiazoles from polymer-bound esters, *Tetrahedron Lett.*, 2004, **45**, 313–316.

27 M. Wang, X. Zhou, Y. Wang, Y. Tian, W. Gou, L. Zhang and C. Li, Direct synthesis of benzothiazoles and benzoxazoles from carboxylic acids utilizing $(o\text{-}CF_3PhO)_3P$ as a coupling reagent, *J. Org. Chem.*, 2024, **89**, 16542–16552.

28 L. M. Bouchet, A. A. Heredia, J. E. Arguello and L. C. Schmidt, Riboflavin as photoredox catalyst in the cyclization of thiobenzanilides: synthesis of 2-substituted benzothiazoles, *Org. Lett.*, 2019, **22**, 610–614.

29 X. Li, Q. Ma, R. Wang, L. Xue, H. Hong, L. Han and N. Zhu, Synthesis of benzothiazole from 2-aminothiophenol and benzaldehyde catalyzed by alkyl carbonic acid, *Phosphorus Sulfur Silicon Relat. Elem.*, 2022, **197**, 689–696.

30 J. Yoo, H. Yuan, H. Miyamura and S. Kobayashi, Facile preparation of 2-substituted benzoxazoles and benzothiazoles via aerobic oxidation of phenolic and thiophenolic imines catalyzed by polymer-incarcerated platinum nanoclusters, *Adv. Synth. Catal.*, 2011, **353**, 3085–3089.

31 X. Zhu, F. Zhang, D. Kuang, G. Deng, Y. Yang, J. Yu and Y. Liang, K_2S as sulfur source and DMSO as carbon source for the synthesis of 2-unsubstituted benzothiazoles, *Org. Lett.*, 2020, **22**, 3789–3793.

32 Y. Riadi, R. Mamouni, R. Azzalou, M. E. Haddad, S. Routier, G. Guillaumet and S. Lazar, An efficient and reusable heterogeneous catalyst animal bone meal for facile synthesis of benzimidazoles, benzoxazoles, and benzothiazoles, *Tetrahedron Lett.*, 2011, **52**, 3492–3495.

33 J. R. Mali, D. V. Jawale, B. S. Londhe and R. A. Mane, An efficient green protocol for the synthesis of 2-aryl substituted benzothiazoles, *Green Chem. Lett. Rev.*, 2010, **3**, 209–212.

34 S. M. Inamdar, V. K. More and S. K. Mandal, CuO nanoparticles supported on silica, a new catalyst for facile synthesis of benzimidazoles, benzothiazoles and benzoxazoles, *Tetrahedron Lett.*, 2013, **54**, 579–583.

35 R. Shelkar, S. Sarode and J. Nagarkar, Nano ceria catalyzed synthesis of substituted benzimidazole, benzothiazole, and benzoxazole in aqueous media, *Tetrahedron Lett.*, 2013, **54**, 6986–6990.

36 S. Das, S. Samanta, S. K. Maji, P. K. Samanta, A. K. Dutta, D. N. Srivastava, B. Adhikary and P. Biswas, Visible-light-driven synthesis of 2-substituted benzothiazoles using CdS nanosphere as heterogeneous recyclable catalyst, *Tetrahedron Lett.*, 2013, **54**, 1090–1096.

37 V. Dixit, G. Kumar, P. Kumar, A. Soni and M. Nemiwal, Emerging strategies for synthesis of heterocyclic compounds enabled by titanium oxide nanoparticles as heterogeneous catalyst, *Tetrahedron*, 2024, **160**, 134039.

38 A. P. Jakhade, M. V. Biware and R. C. Chikate, Two-dimensional Bi_2WO_6 nanosheets as a robust catalyst toward photocyclization, *ACS Omega*, 2017, **2**, 7219–7229.

39 H. Zhao, Y. Zhu, F. Li, R. Hao, S. Wang and L. Guo, A generalized strategy for the synthesis of large-size ultrathin two-dimensional metal oxide nanosheets, *Angew. Chem., Int. Ed.*, 2017, **56**, 8766–8770.

40 G. Zhan and H. C. Zeng, Synthesis and functionalization of oriented metal–organic-framework nanosheets: toward a series of 2D catalysts, *Adv. Funct. Mater.*, 2016, **26**, 3268–3281.

41 X. Dong, Z. Fang, Y. Gu, X. Zhou and C. Tian, Two-dimensional porous Cu–CuO nanosheets: integration of heterojunction and morphology engineering to achieve high-effective and stable reduction of the aromatic nitro-compounds, *Chin. Chem. Lett.*, 2023, **34**, 107295.

42 X. Liu, M. Liu, W. Xu, M. T. Zeng, H. Zhu, C. Z. Chang and Z. B. Dong, An environmentally benign and efficient synthesis of substituted benzothiazole-2-thiols, benzoxazole-2-thiols, and benzimidazoline-2-thiones in water, *Green Chem.*, 2017, **19**, 5591–5598.

43 H. Naeimi and A. Didar, Efficient sonochemical green reaction of aldehyde, thiobarbituric acid and ammonium acetate using magnetically recyclable nanocatalyst in water, *Ultrason. Sonochem.*, 2016, **34**, 889895.

44 M. Khan, *et al.*, CuO nanostructures: facile synthesis and applications for enhanced photodegradation of organic compounds and reduction of p-nitrophenol from aqueous solutions, *RSC Adv.*, 2016, **6**, 56317–56328.

45 T. J. Daou, *et al.*, Copper oxide nanoparticles: synthesis, characterization and optical properties, *J. Mater. Chem.*, 2010, **20**, 8967–8973.

46 H. Bibi, M. Iqbal, H. Wahab, M. Öztürk, F. Ke, Z. Iqbal, M. I. Khan and S. M. Alghanem, Green synthesis of multifunctional carbon coated copper oxide nanosheets and their photocatalytic and antibacterial activities, *Sci. Rep.*, 2021, **11**, 10781.

47 S. Pundir, M. Pal and S. Arora, Facile green synthesis and photocatalytic evaluation of CuO nanostructures under visible light, *Sci. Rep.*, 2023, **13**, 1294.

48 N. A. S. K. Anuar and C. K. Sheng, Structural and morphological characterization of CuO nanostructure precipitated by water-soluble copper(II) nitrate hemi(pentahydrate) and NaOH as reactants, *J. Nano-Electron. Phys.*, 2021, **13**, 05015.

49 (*a*) K. Gopalakrishnan, S. Sudha and R. Rajendran, FTIR analysis and surface morphology of copper oxide nanoparticles synthesized via green route using aqueous leaf extract of Calotropis gigantea, *Mater. Today Proc.*, 2019, **14**, 302–307; (*b*) L. Zhao, Q. Xu and H. Li, Surface

hydroxyl groups and their influence on the performance of CuO-based catalysts in oxidative reactions, *Appl. Surf. Sci.*, 2017, **426**, 206–214.

50 (*a*) S. D. Seo, Y. H. Jin, S. H. Lee, H. W. Shim and D. W. Kim, Low-temperature synthesis of CuO-interlaced nanodiscs for lithium ion battery electrodes, *Nanoscale Res. Lett.*, 2011, **6**, 397; (*b*) S. Sachdeva and I. Choudhary, Photoluminescent characteristics of solution-processed nanoscale copper oxide, *Mater. Phys. Mech.*, 2024, **52**, 27–37.

51 Q. Zhang, K. Zhang, D. Xu, G. Yang, H. Huang, F. Nie, C. Liu and S. Yang, CuO nanostructures: synthesis, characterization, growth mechanisms, fundamental properties and applications, *Prog. Mater. Sci.*, 2014, **60**, 208–337.

52 Y. Moglie, E. Mascaro, F. Zacconi and G. Radivoy, Copper nanoparticles supported on zinc oxide as efficient catalyst for the N-arylation of (hetero)cyclic and acyclic amides, *ChemistrySelect*, 2021, **6**, 4412–4417.

53 H. Naeimi and A. Heidarnezhad, Synthesis of 2-arylbenzothiazoles using nano BF_3/SiO_2 as a reusable and efficient heterogeneous catalyst under mild conditions, *J. Sulfur Chem.*, 2014, **35**, 493–501.

54 A. H. T. Hang, T. L. H. Nguyen, D. K. N. Chau and P. H. Tran, Phosphonium acidic ionic liquid: an efficient and recyclable homogeneous catalyst for the synthesis of 2-arylbenzoxazoles, 2-arylbenzimidazoles and 2-arylbenzothiazoles, *RSC Adv.*, 2018, **8**, 11834–11842.

55 N. N. Pesyan, H. Batmani and F. Havasi, Copper supported on functionalized MCM-41 as a novel and powerful heterogeneous nanocatalyst for the synthesis of benzothiazoles, *Polyhedron*, 2019, **158**, 248–254.

56 N. Hassanloie, N. Noroozi Pesyan, G. Sheykhaghaei, M. Aalinejad, K. Ojaghi Aghbash and H. Alamgholiloo, Preparation of $Fe_3O_4@SiO_2@Cu–MoO_3$ core–shell nanostructures: synergistic effects of copper and molybdenum for catalytic enhancement, *J. Porous Mater.*, 2023, **30**, 859–869.

57 G. Kaur, R. Moudgil, M. Shamim, V. K. Gupta and B. Banerjee, Camphor sulfonic acid catalyzed a simple, facile and general method for the synthesis of 2-arylbenzothiazoles, 2-arylbenzimidazoles and 3H-spiro [benzo[d]thiazole-2,3′-indolin]-2′-ones at room temperature, *Synth. Commun.*, 2021, **51**, 1100–1120.